Biodegradation (2006) 17: 237–250
DOI 10.1007/s10532-005-5019-8

The ACCEL model for accelerating the detoxification kinetics of hydrocarbons requiring initial monooxygenation reactions

Elizabeth P. Dahlen[1,*] & Bruce E. Rittmann[2]
[1]*ChemRisk, Inc. 25 Jessie Street at Ecker Square Suite 1800, San Francisco, CA, 94105-2703, USA;* [2]*Center for Environmental Biotechnology Biodesign Institute at Arizona State University, 1001 South McAllister Avenue, 875701, Tempe, AZ , 85287-5701, USA (*author for correspondence: e-mail: edahlen@chemrisk.com)*

Accepted: 6 April 2005

Key words: activated sludge, dichlorophenol, monooxygenation, nicotinamide adenine dinucleotide, phenolics, specific growth rate

Abstract

The two-tank accelerator/aerator modification of activated sludge significantly increases the biodegradation of hydrocarbons requiring initial monooxygenation reactions, such as phenol and 2,4-dichlorophenol (DCP). The small accelerator tank has a controlled low dissolved oxygen (DO) concentration that can enrich the biomass in NADH + H^+. It also has a very high specific growth rate (μ_{acc}) that up-regulates the biomass's content of the monooxygenase enzyme. Here, we develop and test the ACCEL model, which quantifies all key phenomena taking place when the accelerator/aerator system is used to enhance biodegradation of hydrocarbons requiring initial monooxygenations. Monooxygenation kinetics follow a multiplicative relationship in which the organic substrates (phenol or DCP) and DO have separate Monod terms, while the biomass's content of NADH + H^+ has a first-order term. The monooxygenase enzyme has different affinities (K values) for phenol and DCP. The biomass's NADH + H^+ content is based on a proportioning of NAD(H) according to the relative rates of NADH + H^+ sources and sinks. Biomass synthesis occurs simultaneously through utilization of acetate, phenol, and DCP, but each has its own true yield. The ACCEL model accurately simulates all trends for one-tank and two-tank experiments in which acetate, phenol, and DCP are biodegraded together. In particular, DCP removal is affected most by DO_{acc} and the retention-time ratio, $\Theta_{acc}/\Theta_{total}$. Adding an accelerator tank dramatically increases DCP removal, and the best DCP removal occurs for $0.2 < DO_{acc} < 0.5$ mg/l and $0.08 < \Theta_{acc}/\Theta_{total} < 0.2$. The rates of phenol and DCP utilization follow the multiplicative relationship with a maximum specific rate coefficient proportional to μ_{acc}. Finally, μ_{acc} increases rapidly for $\Theta_{acc}/\Theta_{total} < 0.25$, acetate removal in the accelerator fuels the high μ_{acc}, and the biomass's NADH + H^+ content increases very dramatically for $DO_{acc} < 0.25$ mg/l.

Introduction

For many hydrocarbons, the rate-limiting reaction in their biodegradation is an initial monooxygenation (Gottschalk 1986; Rittmann et al. 1994; Rittmann & McCarty 2001; Sáez & Rittmann 1993). Two examples are the initial monooxygenations of phenol (C_6H_5OH) to catechol ($C_6H_4(OH)_2$) and 2,4-dichlorophenol ($C_6H_3Cl_2OH$) to 3-chlorocatechol ($C_6H_3Cl(OH)_2$):

$$C_6H_5OH + NADH + H^+ + O_2 + M \rightarrow C_6H_4(OH)_2 + NAD^+ + H_2O + M$$

$$C_6H_3Cl_2OH + 2NADH + 2H^+ + O_2 + M \rightarrow C_6H_3Cl(OH)_2 + 2NAD^+ + HCl + H_2O + M$$

in which NAD^+ and NADH + H^+ are the oxidized and reduced forms of nicotinamide adenine dinucleotide, and M is the monooxygenase

enzyme, which is not consumed. In a reactor, the rate of monooxygenation is controlled by the concentration of M, which depends on the concentration of the active biomass and the specific content of the monooxygenase enzyme in the biomass. In addition, the concentration of one or more of its co-substrates can control the monooxygenation rate: the hydrocarbon (e.g., C_6H_5OH or $C_6H_3Cl_2OH$), molecular oxygen (O_2), and intracellular NADH + H^+.

Dahlen & Rittmann (2002a, b) modified the activated sludge process to increase the rate of slow monooxygenation reactions, such as for 2,4-dichlorophenol (DCP). The modification is the two-tank *accelerator/aerator* process, which is illustrated schematically in Figure 1. Influent wastewater and recycled sludge enter a small *accelerator tank* that accelerates monooxygenation kinetics by increasing the cells' intracellular levels of NADH + H^+ and M. The accelerator tank's small volume, high BOD loading, and carefully poised dissolved oxygen (DO) concentration bring about these increases in critical intracellular components. The DO concentration is set low enough to enrich the biomass in NADH + H^+, but not so low that it stops the monooxygenation reaction. In addition, the plug-flow nature introduced by the accelerator tank allows the concentration of the target hydrocarbon (e.g., DCP) to be higher in the accelerator tank than in the aerator, which further accelerates its monooxygenation kinetics in the accelerator tank. Mixed liquor then flows to the *aerator tank*, which has a normal DO concentration for a suspended growth system (>2 mg/l) and is used to ensure complete BOD removal, biomass synthesis, and a proper solids retention time (SRT) (Rittmann & McCarty 2001; Grady et al. 1999).

Dahlen & Rittmann (2002a, b) demonstrated that the two-tank configuration significantly increased the overall removal rates for phenol and 2,4-dichlorophenol (DCP), and they evaluated why the overall rates increased. For the more slowly degraded DCP, the average percentage removal increased from 74% to 93%, even though the detention time of the two-tank system was smaller than that of the one-tank system, because the specific rate of DCP utilization was doubled. The effects of the accelerator tank were systematic and clearly explained why the two-tank system gave improved performance.

(1) Biomass in the accelerator tank was significantly enriched in NADH + H^+ when its DO concentration was below 0.25 mg/l, and the NADH + H^+ concentration had a direct effect on the monooxygenation kinetics.
(2) The main source of NADH + H^+ in the accelerator was oxidation of acetate, a rapidly degraded electron-donor substrate, demonstrating the value of having a rapidly biodegraded primary substrate.
(3) The specific growth rate (μ) was high in the accelerator tank, and the rate coefficients for both monooxygenation reactions were directly proportional to the specific growth rate, supporting that the accelerator tank caused an up-regulation of the biomass's M content.
(4) Monooxygenation rate coefficients in the aerator tank also were much larger than in a one-tank system, even though the specific growth rates were nearly the same; thus, elevated levels of monooxygenase carried over from the accelerator tank to the aerator tank.
(5) The high concentration of DCP in the accelerator tank also was significant for accelerating the monooxygenation reactions there.Our purpose here is to develop and test a mathematical model that represents all the phenomena that we observed with the two-tank system (Dahlen & Rittmann 2002a b), as well as in companion studies with a chemostat (Dahlen & Rittmann 2000). We present the ACCEL model, which describes two tanks in series, each with its own conditions, such as μ and DO concentration. The ACCEL model also describes active biomass and its utilization of and growth on three organic substrates: acetate, a rapidly biodegraded substrate that does not require monooxygenation; phenol, a relatively rapidly degraded aromatic hydrocarbon that requires monooxygenation; and DCP, a slowly biodegraded aromatic hydrocarbon that requires monooxygenation. The ACCEL model simulates the biomass's NADH + H^+ level according to the DO concentration and its specific monooxygenation rate coefficients (representing regulation of M) according to μ in the accelerator tank. We test the ACCEL model to determine how well it captures all the trends found in the experiments of Dahlen & Rittmann (2002a).

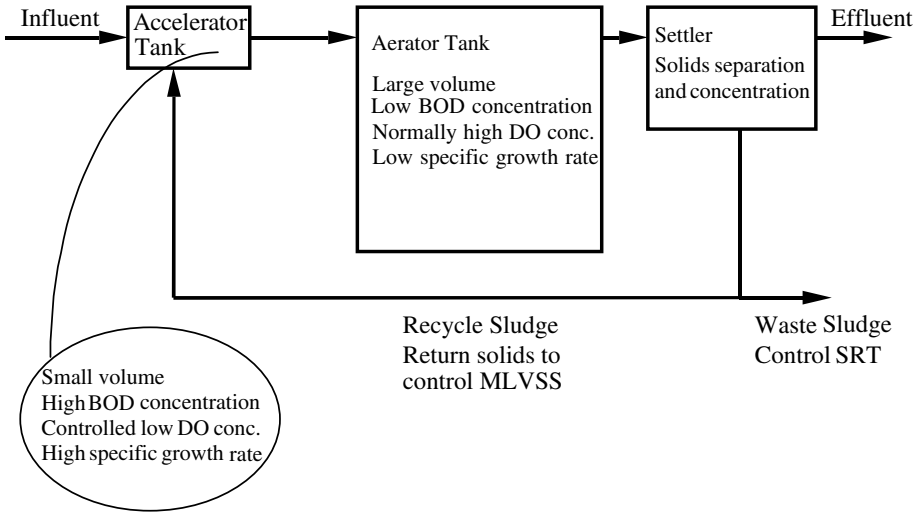

Figure 1. Schematic of the two-tank accelerator/aerator system to accelerate detoxification requiring initial monooxygenation reactions (Dahlen & Rittmann 2002a).

ACCEL-model development

The ACCEL model builds directly on the experimental findings and detailed mechanistic analyses of Dahlen & Rittmann (2000 2002a, b). It synthesizes all the findings into one comprehensive model.

Rates of substrate utilization

The utilization kinetics for phenol and DCP are controlled by their initial monooxygenation reactions. The rate of substrate utilization is affected by the amount of monooxygenase enzyme available, which is directly related to the cell growth rate and differing affinities for specific substrates. Our experimental results demonstrated that, as the growth rate in the tank increased or decreased, the intracellular concentration M changed in a linearly proportional fashion; hence, the specific growth rate must be incorporated as a product in the overall rate expression. In addition, we demonstrated that the enzyme's affinity when processing different substrates had a direct impact on the rate of substrate utilization; as expected, the affinity for phenol was greater than the affinity for DCP (Dahlen & Rittmann 2002a b). All factors controlling monooxygenation rates are shown in Equations (1) and (2).

$$r_{d,l} = \mu \times k_{d,l} \times [X] \times \frac{\left(\frac{[NADH+H^+]}{[X]}\right)}{K_{N,PH} + \left(\frac{[NADH + H^+]}{[X]}\right)} \times \left(\frac{[S_a]}{K'_a + [S_a]}\right) \times \left(\frac{[S_{d,l}]}{K'_{d,l} + [S_{d,l}]}\right) \quad (1)$$

$$r_2 = \mu \times k_2 \times [X] \times \frac{\left(\frac{[NADH+H^+]}{[X]}\right)}{K_{N,DCP} + \left(\frac{[NADH + H^+]}{[X]}\right)} \times \left(\frac{[S_a]}{K'_a + [S_a]}\right) \times \left(\frac{[S_2]}{K'_2 + [S_2]}\right) \quad (2)$$

in which $r_{d,1}$ is the volumetric rate of phenol utilization (gCOD/l*day), r_2 is the volumetric rate of DCP utilization (gCOD(S)/l*day), μ is the specific growth rate (1/day), $k_{d,1}$ is biomass-specific constant for phenol monooxygenation (gCOD/gVSS), k_2 is biomass-specific constant for DCP monooxygenation (gCOD/gVSS), [NADH + H^+] is the reduced-NAD concentration of the biomass (μmolNADH + H^+/l), $K_{N,PH}$ and $K_{N,DCP}$ are the oxygenase molecule's affinity for phenol and

DCP (μmol/l), respectively, [S_a] is the DO concentration (mgDO/l), [S_1] is the phenol concentration (mgCOD/l), [S_2] is the DCP concentration (mgCOD(S)/l), and K_a, K_1, and K_2 are the half-maximum-rate concentrations (mgCOD/l) for DO, phenol, and DCP, respectively. In Equations (1) and (2), the monooxygenation rates are controlled by the concentrations of the monooxygenase enzyme (proportional to μ) and to the concentrations of the hydrocarbon ([$S_{d,1}$] or [S_2]), DO ([S_a]), and intracellular NADH + H^+, each with multiplicative Monod kinetics, since all are co-substrates for the monooxygenase.

The maximum specific rates of phenol and DCP utilization were determined experimentally (Dahlen & Rittmann 2000 2002a) by plotting the rate of substrate utilization versus the product of all other terms on the right-hand side of Equations (1) and (2) divided by the biomass concentration to yield the constants, $k_{d,1}$ and k_2. The slope of the rate of phenol utilization versus the product of the primary donor terms in Equation (1) yields $k_{d,1}$ equal to 6.7 gCOD/gVSS, as shown in Figure 2. In a similar fashion, the rate of DCP utilization versus the product term in Equation (2) yields k_2 equal to 4.7 gCOD/gVSS, as shown in Figure 3.

The rate equations for phenol and DCP utilization incorporate the effects of biomass growth rate, μ, on the monooxygenase level and the Monod term for NADH + H^+ affinity for the monooxygenase enzyme. The cell growth rates in the accelerator tank were substantially higher than the growth rate in the aerator tank where they were nearly constant. The specific growth rates are calculated from mass balances on the biomass flowing into and out of each tank as shown in Equations (3) and (4). Within specific equations that pertain to reactions within the accelerator or the aerator, the subscript 'a' refers to the accelerator tank and 'r' refers to the aerator tank.

$$\mu_a = \frac{(1+r)\times Q\times X^a[t] - Q^r\times Ras}{V_a\times X_a[t]} \qquad (3)$$

$$\mu_r = \frac{(1+r)\times Q}{[X]_{aer}\times V_r}\times\left([X]_{aer}-[X]_{acc}\right) \qquad (4)$$

in which, r is the unitless recycle ratio, which is equal to the recycle flow rate divided by the influent flow rate, Q(l/d), Ras is the biomass concentration in the recycle line (mgVSS/l), V is the volume in the accelerator or aerator tank (l).

The rate expression for acetate utilization, $r_{d,2(a\ or\ r)}$, used in the ACCEL model is shown in Equation (5).

$$r_{d,2} = q_{d,2}\times X\times\frac{S_{d,2}}{K_{d,2}+S_{d,2}} \qquad (5)$$

$S_{d,2}$ is the acetate concentration (mgCOD/l), and X is the concentration of active biomass (mgVSS/l). Since acetate utilization does not require a monooxygenation step, terms involving [NADH + H^+], [S_a], and μ are not necessary, and Equation (5) is a single-Monod expression in which $r_{d,2}$ is the volumetric rate of acetate utilization (gCOD/l*day). Because we did not measure the acetate kinetic parameters, we assume that $q_{d,2}$, the maximum specific rate of acetate utilization, is equal to 3.8 gCOD/gVSS*day and $K_{d,2}$, the half maximum-rate concentration for acetate, is equal to 0.01 mgCOD/l (Pavlostathis & Giraldo-Gomez 1991; Vavilin & Lokshina 1996).

Biomass synthesis and decay

Active biomass is synthesized in proportion to the simultaneous utilizations of acetate, phenol, and DCP, each with its own true yield (mgVSS/mgCOD) (Dahlen & Rittmann 2000 2002b): Y_{PH} for phenol, Y_{DCP} for DCP, and Y_{Ac} for acetate. Active biomass also decays with a first-order endogenous-decay coefficient of b (day^{-1}) (Rittmann & McCarty 2001; Dahlen & Rittmann 2000). Active biomass is not divided into specialized degraders, but utilizes all three substrate together (Dahlen & Rittmann 2000). Therefore, the net growth rate for active biomass in the accelerator tank, $r_{x,a}$ (mgVSS/l*day), is

$$r_{X,a} = X_a[t]\times\frac{(1+r)\times QX_a[t] - Q^r\times Ras}{V_a\times X_a[t]} \qquad (6)$$

where X_a[t] represents the biomass concentration in the accelerator tank and is determined by conducting a mass balance, as shown in the section, mass balances. Q^r is the recycle flow rate and Q is the flow rate through the reactor system.

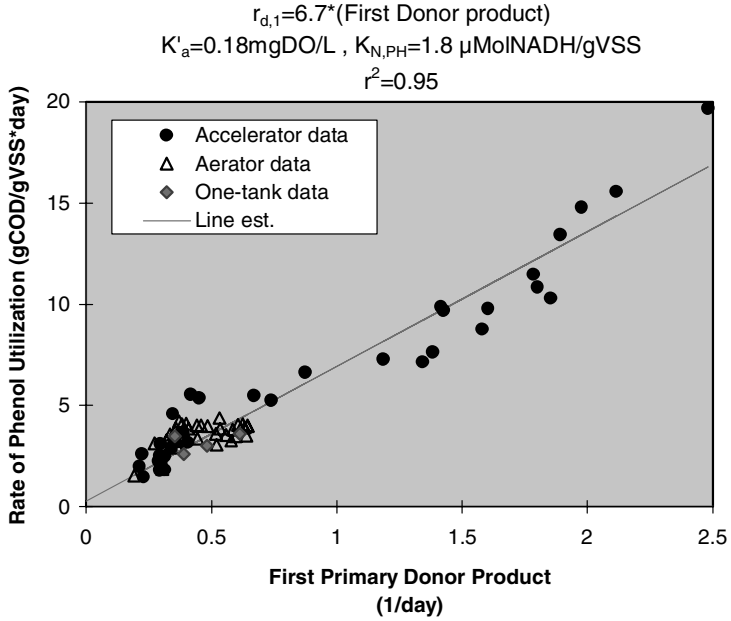

Figure 2. Rate of the first primary donor substrate, phenol, utilization versus the first primary donor product for the accelerator and aerator tanks, and the one-tank system. The first primary donor product is: μ_{acc}*([NADH + H^+]/[X]/$K_{N,PH}$ + [NADH + H^+]/[X])*(DO_{acc}/($\acute{K}_a$ + DO_{acc}))*([$S_{d,1a}$]/($K_{d,1}$ + [$S_{d,1a}$])).

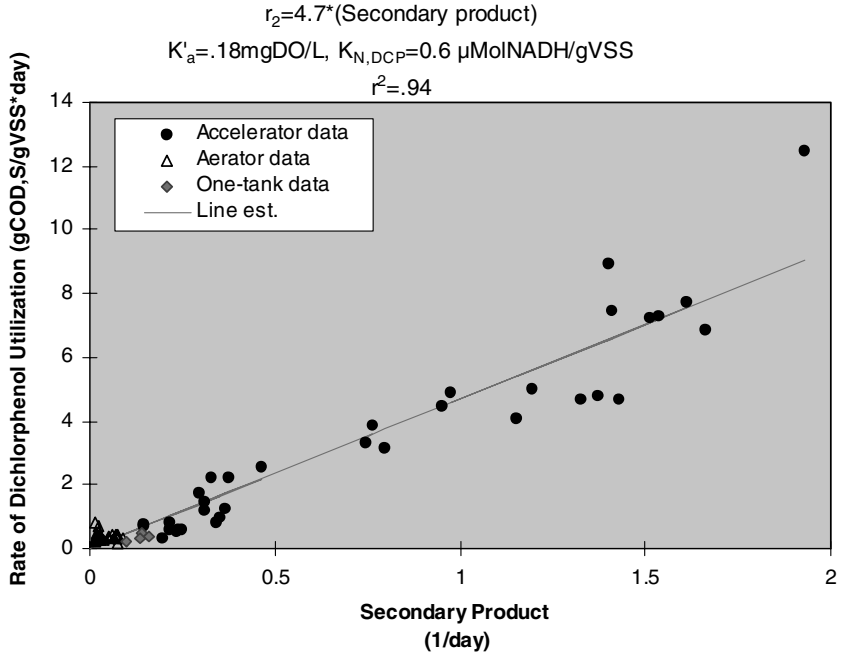

Figure 3. Rate of the secondary substrate, DCP, utilization versus the secondary product term for the accelerator and aerator tanks, and the one-tank system. The secondary product is: μ*([NADH + H^+]/X)/($K_{N,DCP}$ + ([NADH + H^+]/X))*([S_a]/($\acute{K}_a$ + [S_a]))*([S_2]/(K_2 + [S_2])).

Dissolved oxygen

The consumption rate for DO in the accelerator tank is based on a mass balance of all sources and sinks of oxygen demand (Rittmann & McCarty 2001).

$$r_a = r_{d,1_a} + r_{d,2_a} + r_{2a} - r_{Xa} - r_{a,oxyg}. \quad (7)$$

The sinks are the consumption of oxygen demand in phenol, DCP, and acetate, less the oxygen demand of the net biomass synthesis, where all rates are in COD/l*day. In addition, aeration adds DO to the accelerator tank ($r_{a,oxyg.}$).

$NADH + H^+$

The mass balance on NADH + H^+ must include all sources and sinks of electrons: acetate, phenol, DCP, biomass, and DO. Table 1 lists the stoichiometric coefficients for each electron source and sink, and the Greek letters ($\alpha,\alpha',\beta,\beta',\delta,\varepsilon,\gamma$) give the moles of NADH + H^+ consumed or produced per mole of the material in the indicated reaction. Since the initial monooxygenation reactions for phenol and DCP require NADH + H^+, α and β refer to electron sinks for the initial monooxygenation reactions (Dahlen & Rittmann 2002b). Once phenol and DCP have undergone the initial electron-consuming steps (Dahlen & Rittmann 2002b), the remaining electrons released in subsequent hydroxylation and dehydrogenation steps are electron sources and are identified by α and β. Likewise, the stoichiometric parameters for oxidation of acetate (ϵ) is an electron source, while reduction of DO (γ) and production of new biomass (δ) are electron sinks.

The reduced carrier concentration ([NADH + H^+]) varies as the total biomass concentration changes. To capture this phenomenon in our model, we obtain the total concentration of NAD(H) for each tank in our reactor system once the biomass concentration (X_a and X_r) is determined. The reduced carrier concentration is determined by partitioning the total steady state (ss) NAD(H) concentration in the biomass (f = 3.4 μmolNAD(H)/gVSS (Dahlen & Rittmann 2002a)) in proportion to the ratio of source rates to total rates in the accelerator tank, as an example:

$$[\text{NADH} + \text{H}^+]_{a,ss} = \frac{f \times X_a[t] \times [\text{Sum of all Electron Source Rates}]}{[\text{Sum of all Electron Source and Sink Rates}]} \quad (8)$$

where

Sum of all Electron Sink Rates in accelerator

$$= \beta' \times r_{d,1a} + \alpha' \times r_{2a} + \varepsilon \times r_{d,2a} \quad (9)$$

Sum of all Electron Sink Rates in accelerator

$$= \beta \times r_{d,1_a} + \alpha \times r_{2a} + \delta \times r_{Xa} + \gamma \times r_{a_a} \quad (10)$$

Hence, for all rate equations requiring the reduced carrier concentration, this calculated value is an input value that changes with the biomass concentration.

Parameter values

The parameter values for the rate expressions used in the ACCEL model are summarized in Table 2. In order that the ACCEL model have inputs and outputs that are consistent internally and with typically measured quantities, we express all parameters with units of g or mg of chemical oxygen demand (COD) for organic substrates, g or mg of volatile suspended solids (VSS) for biomass, g or mg of dissolved oxygen (DO) for oxygen, and μmol for NAD(H). Unit conversions between moles and grams are 64 gCOD/molAcetate, 224 gCOD/molPhenol, 192 gCOD/molDCP, 160 gCOD/molBiomass, 1.42 gCOD/gVSS, and 8 gDO/molDO (Dahlen & Rittmann 2002b). One important comparison is Table 2 is between the half-maximum-rate concentrations for phenol and DCP: K_1 = 0.8 mgCOD/l for phenol versus K_2 = 14 mgCOD/l for DCP. Because K_2 is 17.5 times larger than K_1, the rate of DCP utilization is much lower than the rate of phenol, particularly when the DCP concentration is low compared to K_2. This is the most important factor in explaining why DCP is biodegraded much more slowly than phenol. The half-maximum rate constants for NADH + H^+ interacting with phenol and DCP, $K_{N,PH}$ and $K_{N,DCP}$, were estimated by varying the

Table 1. Summary of the stoichiometric conversion coefficients for the electron ($NADH + H^+$) sources and sinks

Electron source/sink	Greek letter	Stoichiometric coefficient	Units
Phenol as electron sink	β	1	mol$NADH + H^+$/mol Phenol
Phenol as electron source	β'	11	mol$NADH + H^+$/mol Phenol
DCP as electron sink	α	2	mol$NADH + H^+$/mol DCP
DCP as electron source	α'	10	mol$NADH + H^+$/mol DCP
Acetate	ϵ	4	mol$NADH + H^+$/mol acetate
Biomass	δ	10	mol$NADH + H^+$/mol VSS
DO	γ	2	mol$NADH + H^+$/mol oxygen

respective rate of substrate utilization and comparing that to the cellular growth rate (Dahlen & Rittmann 2002b). The result of this analysis yielded half-maximum growth rate constants that are 1.8 and 0.6 μmol $NADH + H^+$/gVSS for phenol and DCP, respectively. These values indicate that the monooxygenase's affinity for $NADH + H^+$ is greater when DCP is its substrate.

Mass balances

Each reactor in the accelerator/aerator system requires a mass balance on phenol, DCP, acetate, and active biomass. In addition to terms for the microbiological reactions, each mass balance must have terms for advection, which includes the recycle flow from the settler back to the accelerator tank (Figure 1). We assume that the settler has no net biomass accumulation. Table 3 gives the mass balances for each reactor, where subscript a refers to the accelerator tank and subscript r refers to the aerator tank. A total of eight nonlinear ordinary differential equations are required to model the key biochemical reactions in each tank.

Solution technique

Due to the nonlinear rate expressions, the coupled ordinary differential equations in Table 3 cannot be solved in closed form and must be solved numerically. We carried out the numerical solution using *Mathematica* (Wolfram 1994; Bahder 1995), which differs from FORTRAN and C by its ability to handle mathematical expressions, as well as numbers, in an interpretive language. *Mathematica's* numerical differential equation solver, NDSolve, uses an Adams Predictor–Corrector method for non-stiff differential equations and backward difference formulas (Gear Method) for stiff equations. The solver switches between the two methods using heuristics based on an adaptively selected step size. It starts with the non-stiff method and checks for the advisability of switching methods every 10 or 20 steps (Petzold 1983). The solver applies a fourth-order multi-step method, which is advantageous because it uses values obtained in more than one preceding step and solves at a faster rate compared to a one-step method, such as the Runga-Kutta, and is numerically stable (Kreyszig 1993). The solver follows the general procedure of reducing step size until it tracks solutions accurately. To run the model, initial conditions are set for the primary and secondary substrates, as well as the biomass. The model runs until steady state is attained.

Although the ACCEL model was derived for the specific situation of two tanks in series, one substrate requiring no monooxygenation reaction, and two substrates requiring monooxygenations, the model's framework is general and can be extended to other combinations of tanks and substrates. Extension requires following the patterns shown above and making parameter estimates for new substrates.

Modeled system

We solved the ACCEL model to simulate the experimental conditions reported by Dahlen & Rittmann (2002a, b). Table 4 lists the operating conditions that we fixed for simulations. The influent concentrations of phenol, acetate, and DCP represent the average influent concentrations for the five series of experiments (Dahlen & Rittmann 2002a). The DO concentration in the aerator was controlled (by adjusting $r_{r,oxyg.}$) at 6.5 mg/l, which is representative of the average DO concentration in the aerator tank throughout the two-

Table 2. Parameters values used in the ACCEL model

Kinetic parameter	Value	Units	Source
Y_{Ac}	0.42	gVSS/gCOD	1
Y_{PH}	0.30	gVSS/gCOD	1
Y_{DCP}	0.28	gVSS/gCOD	1
b	0.27	Day^{-1}	1
$q_{d,2}$	3.8	gCOD/gVSS-d	4
$k_{d,1}$	6.7	gCOD/gVSS	here
k_2	4.7	gCOD/gVSS	here
$K_{d,1}$	0.80	mgCOD/l	1
$K_{d,2}$	0.01	mgCOD/l	4
K_2	14.0	mgCOD(S)/l	1
K_a	0.02	mgDO/l	2
K'_a	0.18	mgDO/l	2
$K_{N,PH}$	1.80	(μmolNADH + H^+/gVSS	3
$K_{N,DCP}$	0.60	μmolNADH + H^+/gVSS	3
f	3.40	μmolNAD(H)/gVSS	2

Sources: 1 = Dahlen & Rittmann (2000), 2 = Dahlen & Rittmann (2002a), 3 = Dahlen & Rittmann (2002b), and 4 = Pavlostathis & Giraldo-Gomez (1991) and Vavilin & Lokshina (1996).

tank and one-tank experiments, but the DO in the accelerator was varied from 0 to 0.5 mg/l, which spans all but three experiments from the two-tank series. The influent flow rate is the average flow rate from the two-tank and one-tank experiments, 2.4 ml/min. The volume of the aerator was set at its constant value of 900 ml, while the accelerator volume ranged from 58 to 421 ml, which spans the range of retention time ratios for the experiments. The recycle flow ratio is 0.2, which represents the average ratio of the two-tank experiments. The wasting flow rate was set at a constant value of 0.02 ml/min, which is representative of the experimental waste flow rate for the two-tank and one-tank experiments. We set the concentration of the recycled and effluent biomass to match the average concentrations for each series of experiments, which gave a nearly constant solid retention time (SRT) (Rittmann & McCarty 2001) of 32 days.

Table 4 also lists the parameters used for the one-tank simulations. Most notable is the larger aerator volume (1.2 l). We controlled the biomass concentration to give the actual SRT of 40 days. For the one-tank simulations, the influent concentrations were the same as those of the two-tank simulations.

We ran 36 simulations with the ACCEL model for a wide range of accelerator DO concentrations ($r_{a,oxyg}$) and volumes (V_a). We generated the output needed to create 3-dimensional surface plots that could be compared to the corresponding experimental data (Dahlen & Rittmann 2002a).

Results and discussion

The most sensitive output parameter is DCP, for which removals changed markedly as the conditions in the accelerator tank were changed from experiment to experiment (Dahlen & Rittmann 2002a). Table 5 compares the percentage removals and effluent concentrations of DCP between the experimental and model-simulated results. The ACCEL model simulated all DCP removals well. The percent errors between the model simulations and the experimental averages were less than $\pm 1\%$, except for experimental run 3, in which the percent error was 4%. This larger deviation may be due to the fact that run 3 had an influent DCP and phenol concentration above the average values shown in Table 5. Effluent concentrations were similarly close. Even though run 3 had a larger deviation, the model simulation captured the trends that percent DCP removal was much higher than for the one-tank system, but among the least removals for the two-tank system.

We utilized the outputs from all simulations to generate 3-dimensional plots of percent of DCP removed versus the retention time ratio ($\Theta_{acc}/\Theta_{total} = V_a/(V_a + V_r)$) and the DO concentration in the accelerator, DO_{acc}. Figure 5 provides a view of the surface, which highlights trends along each axis and ensures that each of the experimental average data points can be clearly visualized. The 3-dimensional plot also shows the average removal percentages for each series of experiments labeled according to the run number in Dahlen & Rittmann (2002a).

Figure 4 illustrates that the ACCEL model represented the major differences in DCP removal among the experimental runs. For example, runs 1, 2, and 4, which had the highest DCP removal percentage, had the lowest $\Theta_{acc}/\Theta_{total}$ ratios. On the other hand, run 3 had a relatively low DCP-removal percentage because of a combination of small effects from low DO_{acc} and high $\Theta_{acc}/\Theta_{total}$. The steep increase in percent removals as the accelerator DO rises from 0 to 0.2 mg/l shows the positive effect of DO as a co-substrate for the

Table 3. Eight coupled, ordinary, differential mass-balance equations and the settler mass balance that comprise the ACCEL model

Acclerator mass balances:

$$\frac{\partial X_a[t]}{\partial t} = \frac{Q}{V_a} \times r \times Ras + [[(Y_{PH} \times r_{d,1a}) + (Y_{Ac} \times r_{d,2a}) + (Y_{DCP} \times r_{2a})] \times X_a[t]] - b \times X_a[t] - (1 + r) \times \frac{Q}{V_a} \times X_a[t]$$

$$\frac{\partial S_{d,1a}[t]}{\partial t} = \frac{Q}{V_a} \times S_{d,1a}[0] + \frac{Q}{V_a} \times r \times S_{d,1r}[t] - (1 + r) \times \frac{Q}{V_a} \times S_{d,1a}[t] - r_{d,1a}$$

$$\frac{\partial S_{d,2a}[t]}{\partial t} = \frac{Q}{V_a} \times S_{d,2a}[0] + \frac{Q}{V_a} \times r \times S_{d,2r}[t] - (1 + r) \times \frac{Q}{V_a} \times S_{d,2a}[t] - r_{d,2a}$$

$$\frac{\partial S_{2a}[t]}{\partial t} = \frac{Q}{V_a} \times S_{2a}[0] + \frac{Q}{V_a} \times r \times S_{2r}[t] - (1 + r) \times \frac{Q}{V_a} \times S_{2a}[t] - r_{2a}$$

Aerator mass balances:

$$\frac{\partial X_r[t]}{\partial t} = (1 + r) \times \frac{Q}{V_r} \times [X_a[t] - X_r[t]] - \frac{Q_w}{V_r} \times X_r[t] + [(Y_{PH} \times r_{d,1r}) + (Y_{Ac} \times r_{d,2r}) + (Y_{DCP} \times r_{2r})] \times X_r[t] - b \times X_r[t]$$

$$\frac{\partial S_{d,1r}[t]}{\partial t} = (1 + r) \times \frac{Q}{V_r} \times [S_{d,1a}[t] - S_{d,1r}[t] - \frac{Q_w}{V_r} \times S_{d,1r}[t] - r_{d,1r}$$

$$\frac{\partial S_{d,2r}[t]}{\partial t} = (1 + r) \times \frac{Q}{V_r} \times [S_{d,2a}[t] - S_{d,2r}[t] - \frac{Q_w}{V_r} \times S_{d,2r}[t] - r_{d,2r}$$

$$\frac{\partial S_{2r}[t]}{\partial t} = (1 + r) \times \frac{Q}{V_r} \times [S_{2a}[t] - S_{d,2r}[t] - \frac{Q_w}{V_r} \times S_{d,2r}[t] - r_{d,2r}$$

Settler mass balances:

$$(1 + r) \times Q \times X_r[t] = (Q - Q_w) \times X_e[t] + [(r \times Q) + Q_w] \times Ras$$

where Xe represents the biomass concentration in the effluent and is assumed to be 0; thus:

$$Ras = \frac{[(1+r) \times Q] \times X_r[t]}{[(r \times Q) + Q_w]}$$

monooxygenation reaction. As the DO rises beyond about 0.2 mg/l, the effect of DO diminishes, and the removals plateau. As the ratio rises from 0 (no accelerator) to about 0.2, removal dramatically increases, and this increase is optimal at a retention time ratio within a fairly broad range of 0.08–0.2. As the retention time ratio increases above 0.2, removals drop off slightly and then plateau. The model shows that having the accelerator tank dramatically increases DCP removal, but the conditions for the greatest DCP removal are relatively broad.

Dahlen & Rittmann (2002b) demonstrated the importance of a high specific growth rates in the accelerator tank, and this increase was accentuated as the retention time ratio decreased. According to the ACCEL model, DCP removal is accelerated at high μ_{acc}, because the monooxygenase content of the biomass increases with μ_{acc}. To evaluate whether the model properly simulates the large increase in specific growth rate in the accelerator, we plot the average accelerator specific growth rates for each series of experiments and the model-simulated growth rates in Figure 5. The ACCEL

Table 4. Operating conditions used in the ACCEL model simulations

Variable identification	Two-tank system *Input value*	One-tank system *Input value*
X_a initial condition of biomass	10 mgVSS/l	10 mgVSS/l
$S_{d,1}$ phenol input	105 mgCOD/l	105 mgCOD/l
$S_{d,2}$ acetate input	156 mgCOD/l	156 mgCOD/l
S_2 DCP input	15 mgCOD(S)/l	15 mgCOD(S)/l
$r_{r,oxyg.}$ DO in the aerator	6.5 mgDO/l	6.5 mgDO/l
$r_{a,oxyg.}$ DO in the accelerator	0–0.5 mg/l	Not applicable
Q input flow rate	2.4 ml/min	2.4 ml/min
Q_w waste-sludge flow rate	0.02 ml/min	0.02 ml/min
V_r aerator volume	900 ml	1200 ml
V_a accelerator volume	58–421 ml	Not applicable
r recycle ratio	0.2	0.2

model provides nearly a perfect match for the specific growth rate in the accelerator. As the retention-time ratio decreases by decreasing the accelerator volume, the simulated μ_{acc} increases dramatically. The ACCEL model also correctly simulates the specific growth rates in the aerator and one-tank systems, which average 3.0 and 3.5 day^{-1}, respectively.

The specific growth rates are directly tied to the biomass concentrations present in each tank. In order to simulate growth rates that are comparable to the experimental values, the simulated biomass concentrations must also be comparable. As shown in Figure 6, biomass concentrations simulated by the ACCEL model are generally about 35 mgVSS/l in the accelerator tank and 110 mgVSS/l in the aerator tank, values similar to the experimental averages. The solids retention time, Θ_x, which does not vary much from run to run, is controlled by the waste-solids flow rate and concentration, as well as the total mass of cells in the aerator. The concentration of cells in the accelerator is determined by a combination of solids recycle and a high μ_{acc}. With no growth in the accelerator, the biomass concentration there would be about 22 mg/l.

Biomass growth depends on the utilizations of acetate, phenol, and DCP. Because phenol and DCP undergo monooxygenation reactions, the ability of the model to simulate their removal is of great importance. However, acetate removal is critical to the control of the biomass concentration. Figure 7 shows the model-simulated concentrations for acetate, phenol, and DCP in the accelerator tank. Also shown are the experimental data for phenol and DCP. Throughout the simulations, approximately 90% of the acetate is utilized in the accelerator tank, and this percentage rises and falls slightly as the accelerator volume increases or decreases, respectively. Because the removal of acetate remains essentially unchanged in the accelerator tank as the volume changes, the amount of biomass present in the tank remains relatively constant. Thus, acetate biodegradation is key for supporting the high specific growth rate in the accelerator. The model simulates complete removal of acetate from the aerator tank and from the one-tank system. Figure 7 shows that the removals of phenol and DCP are incomplete in the accelerator, and they average approximately 16% and 34%, respectively. The removals of phenol and DCP also vary systematically with the accelerator volume, in agreement with the experimental average values.

Table 5. Comparison of the experimental and model-simulated overall removal percentages for DCP

Run	Retention time ratio $\Theta_{acc}/\Theta_{total}$	DO_{acc} (mg/l)	Percent DCP removed (actual)	Percent DCP removed (model)	Error (%)
1	0.20	0.33	95.9	95.4	−0.4
2	0.10	0.21	95.4	96.0	0.7
3	0.26	0.20	89.2	92.8	4.0
4	0.06	0.50	94.4	94.8	0.5
5	0.32	0.54	92.3	92.6	0.4
6	One-tank	0.00	74.7	74.6	−0.1

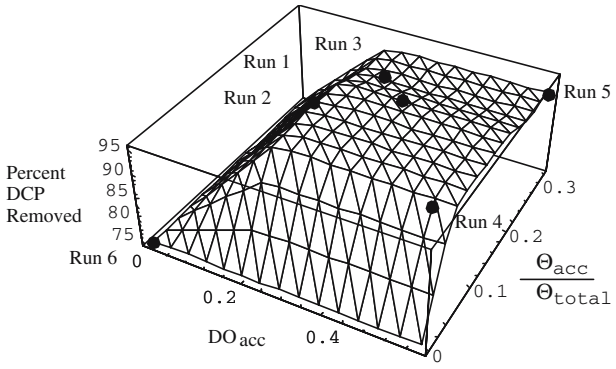

Figure 4. Three-dimensional model-simulated surface for DCP percent removal and the average experimental values plotted as a function of the retention time ratio and the DO concentration in the accelerator.

Dahlen & Rittmann (2002a) demonstrated a strong relationship between the DO and the $NADH + H^+$ concentration in the accelerator. Specifically, a drop in the DO concentration led to a dramatic rise in the $NADH + H^+$ concentration. To evaluate if the ACCEL model captures this trend, we compare the relationships between DO_{acc} and the $NADH + H^+$ concentration in the accelerator for the first experimental series, which was conducted at a retention time ratio of 0.20. In Series 1, the DO concentration in the accelerator ranged from 0.01 to 1.3 mg/l, and the $NADH + H^+$ concentration rose sharply as the DO concentration fell. We ran the model using the same input parameters as those measured for each experimental run in the series (Dahlen & Rittmann 2002a). The physical parameters are similar to those presented in Table 4.

For each experimental run within Series 1, Figure 8 plots the model-simulated $NADH + H^+$ concentration and the experimental value against the DO concentration in the accelerator. The model accurately captures the trend of increasing $NADH + H^+$ concentration with decreasing DO concentration. This indicates that the partitioning of NAD(H) based on the rate

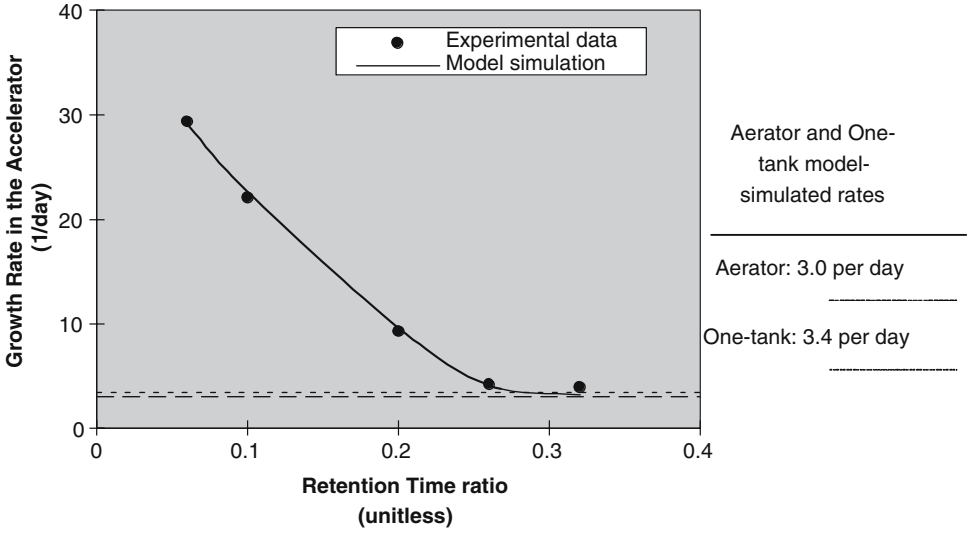

Figure 5. Comparison between the model-simulated specific growth rates in the accelerator tank (μ_{acc}) to the average experimental values.

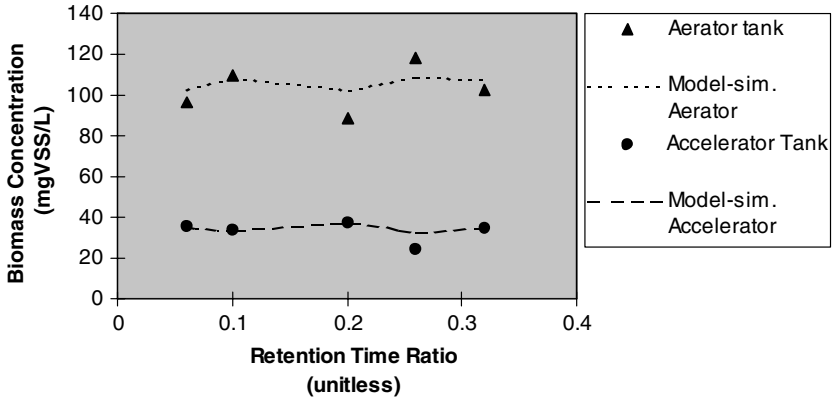

Figure 6. Comparison of the model-simulated to average experimental biomass concentrations (X_a) in the accelerator and aerator tanks for each series.

of NADH + H^+ sources normalized to all source and sink rates (Equations (8–10)) accurately reflects the accelerator tank trends observed during the experiments when DO was very low. The model-simulated aerator NADH + H^+ concentrations vary only slightly and average about 1.0 μmolNADH + H^+/gVSS, and the level was 1.4 μmolNADH + H^+/gVSS in the one-tank simulation; both are similar to the experimental average values.

The rates of the monooxygenation reactions in the accelerator tank should be significantly higher than those in the aerator tank (Dahlen & Rittmann 2002a). This increase in rate is a composite effect from the concentrations of the substrate and DO, as well as from the cells' specific growth rate and NADH + H^+ level. Figures 9 and 10 compare the experimental and simulated rates for phenol and DCP removals, respectively, for Series 1. Both rates are plotted against the product of the normalized NADH + H^+ concentration and the Monod functions for DO and the phenolic substrate (Equations (1–3)). The simulated rates of removal for phenol and DCP show positive trends that match the experimental data. Because the specific growth rate did not vary significantly in this series, the data in Figures 9 and 10 do not test the μ effect by comparison among them. On the other hand, the absolute value of the rate depends on the μ_{acc} value of the series; the good match for DCP removals across the series (Table 5 and Figure 4) show that the μ effect on the monooxygenase level also is captured correctly.

Conclusions

The ACCEL model synthesized and quantifies all key phenomena that occur when the two-tank accelerator/aerator system is used to enhance biodegradation of hydrocarbons that require initial monooxygenation reactions. Critical phenomena are represented in the following ways:

- The kinetics of monooxygenation reactions (Equations (1) and (2)) follow a multiplicative relationship in which the organic substrates (phenol or DCP), the biomass's content of NADH + H^+, and dissolved oxygen have separate Monod terms. The monooxygenase enzyme has different affinities (K values) for phenol and DCP.
- The rates of phenol and DCP utilization followed the multiplicative relationship with a maximum specific rate coefficient proportional to μ_a, which represents up-regulation of the monooxygenase.
- The monooxygenase enzyme had different affinities for NADH + H^+ when it reacted with phenol versus DCP.
- The biomass's NADH + H^+ content is based on a proportioning of NAD(H) according to the relative rates of NADH + H^+ sources and sinks (Equation (8)).
- Biomass synthesis occurs simultaneously through utilization of acetate, phenol, and DCP, but each has its own true yield value.

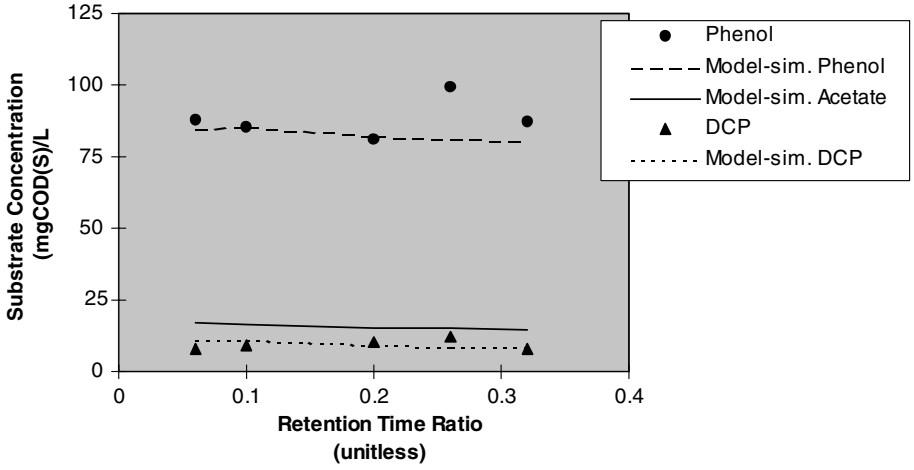

Figure 7. Model-simulated concentrations of acetate, phenol, and DCP in the accelerator tank and experimental average phenol and DCP concentrations.

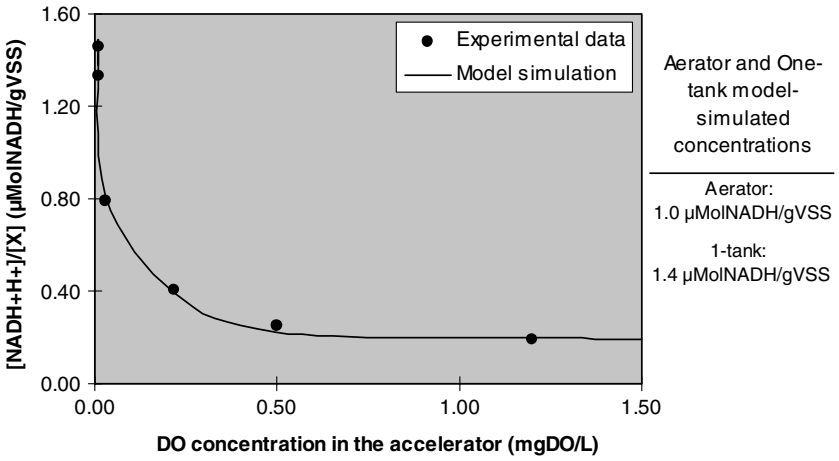

Figure 8. Comparison of the model-simulated reduced carrier concentration versus the actual measurements in the accelerator tank for the experimental series one, retention time ratio 0.20 (Series 1 of Dahlen & Rittmann, 2002a).

- The ACCEL model accurately simulates the results from our series of one-tank and two-tank experiments in which acetate, phenol, and DCP were biodegraded together. In particular, the model correctly captured these trends:
- The removal of DCP is affected by DO_a and Θ_a/Θ_{total}.
- Having an accelerator tank causes a dramatic increase in DCP removal.
- For these experiments, the best DCP removal occurs for $0.2 < DO_a < 0.5$ mg/l and $0.08 < \Theta_a/\Theta_{total} < 0.2$.
- Most acetate removal occurs in the accelerator, and this fuels the high μ_a. However, most removals of phenol and DCP occur in the aerator tank.
- The specific growth rate in the accelerator tank (μ_{acc}) increases rapidly for $\Theta_a/\Theta_{total} < 0.25$.

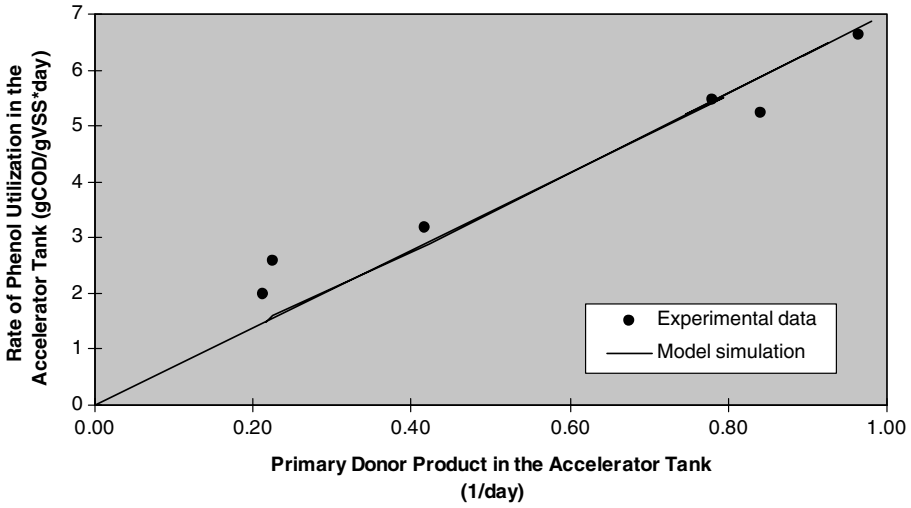

Figure 9. Comparison of the model-simulated rate of phenol removal in the accelerator tank to the experimental values plotted against the primary donor product, μ_{acc}*([NADH + H^+]/[X]/$K_{N,PH}$+[NADH + H^+]/[X])*(DO_{acc}/($\acute{K}_a + DO_{acc}$))*([$S_{d,1a}$]/($K_{d,1}$+[$S_{d,1a}$])).

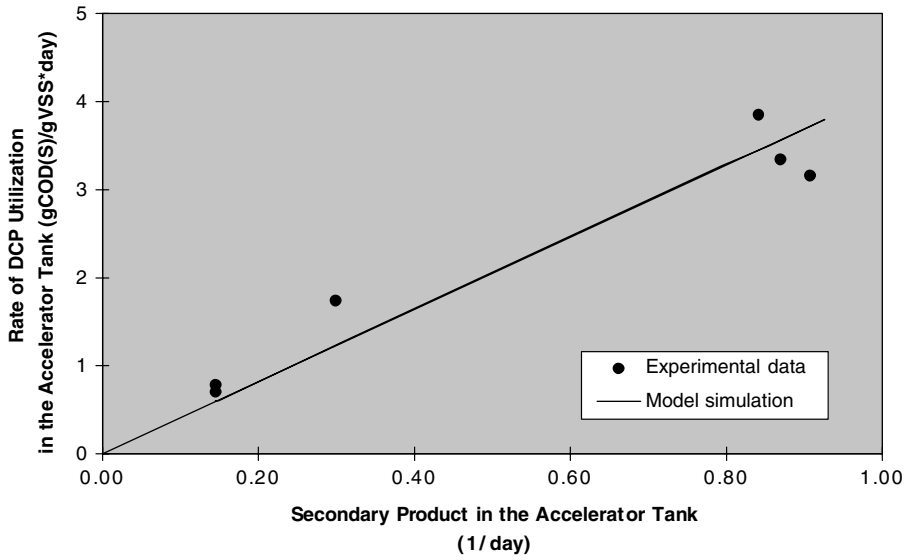

Figure 10. Comparison of the model-simulated rate of DCP removal in the accelerator tank to the experimental values plotted against the secondary product, μ_{acc}*([NADH + H^+]/[X]/$K_{N,DCP}$ + [NADH + H^+]/[X])*(DO_{acc}/($\acute{K}_a$ + DO_{acc}))*([S_{2a}]/(K_2 + [S_{2a}])).

- The biomass's NADH + H^+ content increases very dramatically for DO_a < 0.25 mg/l.
- The high growth rate in the accelerator tank diverted a large flow of electrons to synthesis and this was the primary cause for the lower NADH + H^+ content in the accelerator.

Acknowledgements

The authors acknowledge financial support of the United States National Science Foundation through grant number BES9413824. The authors also want to acknowledge Northwestern University Department of Civil and Environmental Engineering where this research work was conducted.

References

Bahder TB (1995) Mathematica for Scientists and Engineers. Addison-Wesley Publishing Co., Inc., New York

Dahlen, EP, 1999. Accelerating Detoxification by Manipulating Intracellular Electron Carriers, Ph.D. dissertation, Dept. of Civil Engineering, Northwestern University, Evanston, IL, USA

Dahlen E. P. & Rittmann B. E. (2000) Analysis of oxygenation reactions in a multi-substrate system – a new approach for estimating substrate-specific true yields. Biotechnol. Bioeng. 70: 685–692

Dahlen EP & Rittmann BE (2002b) A detailed analysis of the mechanisms controlling the acceleration of 2.4-DCP monooxygenation in the two-tank suspended growth process. Biodegradation 13: 117–130

Gottschalk G. (1986) Bacterial Metabolism, . 2nd. edn. Springer-Verlag, Inc., New York

Grady CPL, Daigger GT & Lim HC (1999) Biological Wastewater Treatment. 2nd edn.Marcel Dekker, Inc., New York

Kreyszig E (1993) Advanced Engineering Mathematics. 7th edn.John Wiley and Sons, Inc., New York

Pavlostathis SG & Giraldo-Gomez E (1991) Kinetics of anaerobic treatment: A Critical Review. Crit. Rev. Env. Contr. 21(5/6): 411–490

Petzold LR (1983) Automatic selection of methods for solving stiff and nonstiff systems of ordinary differential equations. SIAM J. Sci. Stat. Comp. 4: 136–148

Rittmann BE & McCarty. PL (2001) Environmental Biotechnology: Principles and Applications. McGraw-Hill Book Co., New York

Rittmann BE, Seagren E, Wrenn BA, Valocchi AJ, Ray C & Raskin L (1994) In Situ Bioremediation. 2nd editionNoyes Publishers, Inc., Park Ridge, NJ, USA

Sáez PB & Rittmann BE (1993) Biodegradation kinetics of a mixture containing a primary substrate (phenol) and an inhibitory co-metabolite (4-chlorophenol). Biodegradation 4: 3–21

Wolfram S (1994) Mathematica, the Student Book. Addison-Wesley Publishing Co., Inc., New York